

# A Conservative Variational Method for Multicomponent Concentration Time Dependent Diffusion

CLARENCE E. LEE\* AND BRUCE C. WILSON

*Department of Nuclear Engineering, Texas A & M University,  
College Station, Texas 77843*

Received February 28, 1984; revised August 28, 1984

The multicomponent multiregion time dependent concentration diffusion-decay equation with sources is solved using a variational technique. A Lagrangian constraint is appended to the variational functional to ensure a physically correct solution to the balance equations. Spatial dependence of the diffusional coefficients is allowed between nodal values. Solutions have continuity of concentration and mass flux at material interfaces. The resultant time dependent nodal equations are solved by an exponential matrix method. Comparison with simple analytic solutions indicates that accurate physical results are obtained for few nodal values per material and that convergence is of order  $O(h^6)$ . With minor modification the methodology is applicable to multigroup time dependent neutron diffusion, and two solutions are compared. © 1985 Academic Press, Inc.

## INTRODUCTION

In this paper we investigate the variational solution of multicomponent concentration,  $C(r, t)$ , time dependent diffusion governed by Fickian currents,  $\mathbf{J} = -[D] \text{grad } C$ , a linear decay (or production) term,  $[L] C$ , and a source,  $S$ , which satisfies the balance equation

$$\partial C(r, t) / \partial t = \text{div} [D(r)] \text{grad } C(r, t) - [L(r)] C(r, t) + S(r, t). \quad (1)$$

In the case of binary diffusion of fission products, for example, the matrix diffusion coefficients,  $[D]$ , can depend non-linearly on the temperature and concentrations. In this analysis, however, we assume that a spatial representation of  $[D]$  is valid over a suitably chosen sub-domain during the time of interest. Additionally, we assume that the matrix  $[D]$  is in diagonal form,  $[D] = D_{nm} \delta_{nm}$ , where  $\delta_{nm}$  is the Kroenecker delta,  $1 \leq n, m \leq M$ , where  $M$  is the number of components. Extensions to non-diagonal non-singular forms of  $[D]$  are straightforward. For fission product diffusion,  $[L]$  is usually the constant decay-production matrix.

\* Present address: Technadyne Engineering Consultants, P.O. Box 13928 Albuquerque, N. Mex. 87192.

Applications to multigroup neutron diffusion can also be obtained from Eq. (1) by modifying the time rate of change term to  $(1/v) \partial C / \partial t$ , where  $C$  is redefined to be the neutron flux, and  $v$  is the neutron velocity. The matrix  $[D]$  then becomes the multigroup neutron diffusion coefficient matrix, and the  $[L]$  matrix includes the macroscopic cross sections from removal, fission, and scattering [1], which could exhibit spatial dependence due to burnup. Thus, the matrix elements of  $[D]$  and  $[L]$  are allowed to be spatially dependent.

Finite difference (FD) solutions have been developed for Eq. (1) at a finite number of spatial nodes [1-4]. Time step discretization methods may require small time steps in order to avoid instabilities and/or inaccuracies, especially if the resultant equations are tightly coupled or stiff [1, 3]. Even with continuous time solutions, as used in the DASH FD program [2], the second order FD spatial representations may require a large number of carefully placed nodes to obtain accurate concentration gradient estimates near exterior boundaries, as is needed to predict the fission product mass flux from a fuel element [3, 4].

Variational, Galerkin, or finite element methods can also be used to derive nodal representations of the diffusion equation [1, 5, 6]. With the success of variational methods for steady state neutron diffusion problems [7], extensions to time dependent diffusion solutions are of interest. A variational functional is minimized with respect to trial function coefficients in order to obtain the time dependent nodal equations. The trial functions are chosen to satisfy certain conditions. In multimedia problems concentration and flux continuity are frequently appropriate interface boundary conditions. (Concentration jumps can occur for metallic fission products at gaps or material interfaces due to a non-linear concentration dependence of the thermodynamic potential, but that problem will be addressed elsewhere.) A unique polynomial trial function can be determined by applying continuity of  $C$  and  $J$  at material interfaces: cubic hermite polynomial shape functions result. Mixed homogeneous or inhomogeneous exterior boundary conditions are imposed by lagrangian constraints.

After minimization of the variational functional with respect to the nodal components, the resultant time dependent matrix initial value equations are solved using exponential matrix techniques [8]. The matrix solution method has analytic accuracy in the time variable and is well suited to solve the stiff equations sometimes encountered. The continuous spatial solutions between nodes are evaluated by interpolation of the trial function.

Solutions of the time dependent nodal equations will not necessarily satisfy the balance equation, Eq. (1), in a spatial integral sense unless a Lagrange multiplier term is appended to the variational functional, as was observed in steady state solutions [7]. Without the constraint, for a single isotope, this method is equivalent to the Galerkin method.

The results of imposing the conservation constraint are compared with analytic solutions. Without the constraint, in addition to the solutions not satisfying the governing balance equation in an integral sense at a particular time, late time solutions (essentially) near steady state yield a fictitious non-decreasing volume

integrated time rate of change, instead of a value approaching zero, as should be obtained. On the other hand, with the constraint, the conservation variational method provides an accurate and physically correct solution with significantly fewer nodes than FD methods. The FD solutions are conservative and evaluated by the same matrix operator method [2, 8].

Four simple concentration diffusion-decay problems are addressed in one dimensional geometries, for one and two-component and one- and two-medium problems, including fission product diffusion in an HTR pebble bed fuel element. Reasonably accurate time dependent concentration solutions are obtained even for very few nodes/material (2 nodes = 3–5%; 3 nodes = 0.1–0.3%; 4 nodes = 0.01–0.05%). The maximum errors in the system are quoted relative to analytical solutions. Balance is exact and calculated leakages are accurate. The apparent spatial convergence rate of these simple problems is  $O(h^6)$  in cell size  $h$ . We also compare two late time neutron flux diffusion solutions with critical eigenvalue steady state results. This computation involves completely multicomponent (multigroup) multiregion equations.

#### MODEL DEVELOPMENT OF THE VARIATIONAL FUNCTIONAL

The time dependent diffusion equation can be solved by a variational method if there is a functional,  $I(w)$ , such that  $\mathbf{C}(r, t)$ , which satisfies Eq. (1), is the necessary condition for the functional to be an extremum [5]. The functional in one-dimensional geometries for which  $\mathbf{w}(r, t)$  obeys the diffusion equation is

$$I(\mathbf{w}, \mathbf{w}^+) = \langle \mathbf{w}^+, \partial \mathbf{w} / \partial t - \text{div} [D] \text{grad } \mathbf{w} + [L] \mathbf{w} - \mathbf{S} \rangle - \langle \mathbf{S}^+, \mathbf{w} \rangle \quad (2a)$$

$$\begin{aligned} &= \langle \mathbf{w}^+, \partial \mathbf{w} / \partial t \rangle + \langle \partial \mathbf{w}^+ / \partial r, [D] \partial \mathbf{w} / \partial r \rangle \\ &+ \langle \mathbf{w}^+, [L] \mathbf{w} \rangle - \langle \mathbf{w}^+, \mathbf{S} \rangle - \langle \mathbf{S}^+, \mathbf{w} \rangle \end{aligned} \quad (2b)$$

and the trial function  $\mathbf{w}$  and its adjoint  $\mathbf{w}^+$  are real valued functions on  $[a, b]$  with  $\mathbf{w}, \mathbf{w}^+$ , and their derivatives belonging to  $L^2[a, b]$ . We define

$$\langle f, g \rangle = k(c) \int_0^T \int_a^b f(r) g(r) r^c dr dt, \quad (3)$$

where the coefficient  $k(c) = 1, 2\pi,$  and  $4\pi$  for  $c = 0, 1,$  and  $2$  in slab, cylindrical, or spherical geometry, respectively. Applying the Euler-Lagrange equation for Eq. (2) yields Eq. (1). The exterior boundary conditions of the original problem are appended to Eq. (2) as a constraint.

In developing numerical solutions the interval  $[a, b]$  is divided into  $I$  mesh cells, each of which can have different material properties. The spatial continuity of  $\mathbf{w}$  and (the current)  $\mathbf{J}(r) = -[D(r)] \partial \mathbf{w}(r) / \partial r$  (and adjoints) at internal material interfaces is assumed. In each cell there are four continuity conditions (two at each cell

edge). Assuming a polynomial trial function a cubic representation can be found which exactly satisfies the continuity conditions. We impose the internal continuity conditions

$$\mathbf{w}(r_{i-}) = \mathbf{w}(r_{i+}), \quad (4)$$

$$-\mathbf{J}_{i-} = [D(r_{i-})] \partial \mathbf{w}(r_{i-}) / \partial r = [D(r_{i+})] \partial \mathbf{w}(r_{i+}) / \partial r = -\mathbf{J}_{i+} \quad (5)$$

where the ( $\pm$ ) appended to the nodal coordinate,  $r_i$ , indicates evaluation from the left ( $-$ ) or right ( $+$ ). The trial function which interpolates the parameters and satisfies the continuity conditions is [6]

$$\begin{aligned} \mathbf{h}_i(r, t) = & \mathbf{C}_i s_0(1-p) + \mathbf{C}_{i+1} s_0(p) \\ & - K_i [D(r_{i+})]^{-1} \mathbf{J}_i s_1(1-p) + K_i [D(r_{i+1-})]^{-1} \mathbf{J}_{i+1} s_1(p), \end{aligned} \quad (6)$$

where we have defined the variables

$$K_i = r_{i+1} - r_i, \quad p = (r - r_i) / K_i, \quad 0 \leq p \leq 1, \quad (7)$$

and the hermite polynomials

$$s_0(p) = p^2(3 - 2p), \quad s_1(p) = p^2(1 - p). \quad (8)$$

The concentration,  $\mathbf{C}_i(t)$ , and current,  $\mathbf{J}_i(t)$ , are real interpolating parameters defined at  $r_i$ ,  $1 \leq i \leq I$ . The corresponding adjoint trial function,  $\mathbf{h}_i^+(r, t)$ , has a similar form.

A set of time dependent matrix equations is obtained in terms of  $\mathbf{C}_i(t)$  and  $\mathbf{J}_i(t)$  by substituting Eq. (6), and its adjoint, into the functional and taking the variation of the result with respect to  $\mathbf{C}_i^+$  and  $\mathbf{J}_i^+$ .

If steady state solutions exist for the time dependent problem, the late time solutions should approach the steady state solution. For steady state multigroup neutron diffusion solutions from such a variational formulation it was observed that the equations would not conserve (balance) over a mesh cell or in the system [7]. However, conservation is obtained by construction for proper FD representations [3, 4]. Since the diffusion equation is a balance relation, particles (the diffusing field) must be conserved. Therefore, in order to obtain cell-wise conservation, a Lagrange multiplier term is appended to the functional,  $I(\mathbf{w}, \mathbf{w}^+)$ , which subjects solutions to the constraint of conservation. The appropriate time dependent conservation equation is obtained by substituting the trial function into the diffusion equation and integrating over the cell, with the result

$$\langle 1, \partial \mathbf{h}_i / \partial t \rangle = A_i \mathbf{J}_i - A_{i+1} \mathbf{J}_{i+1} - \langle 1, [L_i(p)] \mathbf{h}_i(p) \rangle + \langle 1, \mathbf{S}_i(p) \rangle. \quad (9)$$

Here  $A_i$  is the surface area normal to node  $i$ , and  $A_i \mathbf{J}_i - A_{i+1} \mathbf{J}_{i+1}$  results from Gauss' divergence theorem applied to the leakage term in Eq. (1).

Substituting the trial functions  $\mathbf{h}_i(p, t)$  and  $\mathbf{h}_i^+(p, t)$  into Eq. (2) and defining

$\mathbf{E}_i^+(t)$  and  $\mathbf{E}_i(t)$  as the Lagrange multipliers for imposing cell-wise conservation constraint, the conservational functional becomes

$$I_1(\mathbf{w}, \mathbf{w}^+) = \sum_1^I I_i(\mathbf{w}, \mathbf{w}^+), \quad (10a)$$

where

$$\begin{aligned} I_i(\mathbf{w}, \mathbf{w}^+) = & \langle \mathbf{h}_i^+(p), \partial \mathbf{h}_i(p)/\partial t \rangle + (1/K_i^2) \langle \partial \mathbf{h}_i^+(p)/\partial p, [D_i(p)] \partial \mathbf{h}_i(p)/\partial p \rangle \\ & + \langle \mathbf{h}_i^+(p), [L_i(p)] \mathbf{h}_i(p) \rangle - \langle \mathbf{h}_i^+(p), \mathbf{S}_i(p) \rangle \\ & + \langle \mathbf{E}_i^+, \partial \mathbf{h}_i(p)/\partial t + [L_i(p)] \mathbf{h}_i(p) - \mathbf{S}_i(p) \rangle \\ & + E_i^+ (-A_i \mathbf{J}_i + A_{i+1} \mathbf{J}_{i+1}) \\ & + \langle \mathbf{E}_i, -\partial \mathbf{h}_i^+(p)/\partial t + [L_i(p)]^+ \mathbf{h}_i^+(p) - \mathbf{S}_i^+(p) \rangle \\ & + E_i (-A_i \mathbf{J}_i^+ + A_{i+1} \mathbf{J}_{i+1}^+) \end{aligned} \quad (10b)$$

and

$$\langle f_i(p), g_i(p) \rangle = k(c) \int_0^T \int_0^1 f_i(p) g_i(p) (K_i p + r_i)^c dp dt. \quad (10c)$$

Minimizing the functional  $I_1$  with respect to  $\mathbf{C}_i^+$ ,  $\mathbf{J}_i^+$ ,  $\mathbf{E}_i^+$ ,  $\mathbf{C}_i$ ,  $\mathbf{J}_i$ , and  $\mathbf{E}_i$  results in time dependent matrix equations for the nodal components that satisfy the continuity of concentration and current boundary conditions at material interfaces, and the conservational relationship.

For the exterior boundary conditions we impose an additional constraint at the left and right hand boundaries which allows for the boundary condition [1]

$$[a_1] \mathbf{C}(0, t) + [a_2] \partial \mathbf{C}(0, t)/\partial p = \mathbf{a}_3,$$

and

$$[b_1] \mathbf{C}(1, t) + [b_2] \partial \mathbf{C}(1, t)/\partial p = \mathbf{b}_3, \quad (11)$$

where  $[a_i]$  and  $[b_i]$ ,  $i = 1, 2$ , are diagonal matrices, and  $\mathbf{a}_3$  and  $\mathbf{b}_3$  are vector constants. The exterior boundary conditions are treated in the matrix solutions below by imposing the equations

$$\partial/\partial t ([a_1] \mathbf{C}_1(t) + [a_2] [D_1(0)]^{-1} \mathbf{J}_1(t)) = 0,$$

and

$$\partial/\partial t ([b_1] \mathbf{C}_{I+1}(t) + [b_2] [D_{I+1}(1)]^{-1} \mathbf{J}_{I+1}(t)) = 0, \quad (12)$$

at the boundaries, where the initial condition vector is set to  $\mathbf{a}_3$  or  $\mathbf{b}_3$  on the left and right boundaries, respectively. For the problems addressed in this paper, we use

$\mathbf{a}_3 = \mathbf{b}_3 = 0$  (homogeneous),  $[a_1] = 0$  (Neumann), and  $[b_2] = 0$  (Dirichlet) corresponding to symmetry (zero current) at the origin and zero concentration at the outside boundary.

### TIME DEPENDENT MATRIX SOLUTIONS

The matrix equations resulting from the variational formulation are

$$[T] d\mathbf{X}/dt = [A] \mathbf{X} + \mathbf{S}, \quad (13)$$

where  $[T]$  and  $[A]$  are symmetric block tridiagonal matrices, given in the Appendix. The solution vector  $\mathbf{X} = [X_1, \dots, X_{I+1}]^T$  for  $I$  cells ( $I+1$  nodes), where  $X_i = [C_{i,1}, J_{i,1}, E_{i,1}, \dots, C_{i,M}, J_{i,M}, E_{i,M}]^T$  is of length  $3M$ , contains components of the nodal concentration  $C_{i,m}$ , current,  $J_{i,m}$ , and (conservation) Lagrange multiplier,  $E_{i,m}$ , for node  $i$ , and component  $m$ ,  $1 \leq m \leq M$ . For nonconservational calculations, the components  $E_{i,m}$  are omitted. In FD formulations, only the components  $C_{i,m}$  occur, the matrix  $[T]$  is diagonal, and  $[A]$  is tridiagonal [1, 3, 4].

Since the matrix  $[T]$  is nonsingular, Eq. (13) is equivalent to

$$d\mathbf{X}/dt = [T]^{-1}[A] \mathbf{X} + [T]^{-1} \mathbf{S}. \quad (14)$$

If the matrix  $[B] = [T]^{-1}[A]$  is constant over a time interval  $(0, t)$ , Eq. (14) can be solved using the methods of ASH[8], an analytic matrix technique based on the Volterra calculus [9]. Further, if the source is described by  $\mathbf{S}(t') = \mathbf{S}_1 + t'\mathbf{S}_2$  on  $(0, t)$ , with  $\mathbf{S}_0$  and  $\mathbf{S}_1$  constant, then the solution is

$$\mathbf{X}(t) = e^{[B]t} \mathbf{X}(0) + t\mathbf{D}([B]t)[T]^{-1} \mathbf{S}_0 + t^2\mathbf{Z}([B]t)[T]^{-1} \mathbf{S}_1, \quad (15)$$

where the exponential matrix operator is

$$e^{[B]t} = \sum_{n=0}^{\infty} ([B]t)^n/n!, \quad (16)$$

and the matrix operators  $\mathbf{D}([B]t)$  and  $\mathbf{Z}([B]t)$  are

$$\mathbf{D}([B]t) = ([B]t)^{-1}(e^{[B]t} - I) = \sum_{n=0}^{\infty} ([B]t)^n/(n+1)!,$$

and

$$\mathbf{Z}([B]t) = ([B]t)^{-1}(\mathbf{D}([B]t) - I) = \sum_{n=0}^{\infty} ([B]t)^n/(n+2)!, \quad (17)$$

forms which exist even if the matrix  $[B]$  is singular.

Direct evaluation of the matrices  $e^{[B]t}$ ,  $\mathbf{D}([B]t)$ , and  $\mathbf{Z}([B]t)$  can lead to numerical difficulties if the magnitude of the eigenvalues of  $[B]t$  are greater than

unity. The eigenvalues are scaled to be less than unity by forming  $H = 2^{-p}[Bt]$ , with the integer  $p$  determined such that the norm  $\|H\| = \frac{1}{2}$ , which is satisfied provided

$$p \geq 1 + \ln \left( \sum_{jk} H_{jk}^2 \right) / 2 \ln 2 \quad (18)$$

The numerical evaluation of  $e^{[H]}$ ,  $D([H])$ , and  $Z([H])$  is performed using a finite number of terms,  $N$ , of the corresponding series representation, where  $N$  is chosen dynamically such that the remainder terms have norm less than a some prescribed error. Knowing  $e^{[H]}$ ,  $D([H])$ , and  $Z([H])$ , the values of  $e^{([B]t)}$ ,  $D([B]t)$ , and  $Z([B]t)$  are obtained by scaling the matrix functions of  $[H]$  upwards by powers of 2, until  $[B]t = 2^p[H]$ , with the recursion relations

$$D(2^{p+1}[H]) = D(2^p[H]) \left[ I + \frac{1}{2}(2^p[H]) D(2^p[H]) \right],$$

and (19)

$$Z(2^{p+1}[H]) = \frac{1}{2}Z(2^p[H]) + \frac{1}{4}[D(2^p[H])]^2,$$

which can be proved by induction arguments [8].

The SPLASH program was developed to solve this time dependent multicomponent multiregion one-dimensional diffusion decay problem [10, 11].

## RESULTS

Detailed comparisons with analytical and finite difference solutions have been made. In one dimension, typical one or two component, and one or two media problems are evaluated from initial to (essentially) steady state rapidly with few nodes/material and reasonable accuracy compared to analytical solutions (2 nodes = 3–5%; 3 nodes = 0.1–0.3%; 4 nodes = 0.01–0.03%). Balance is exact; leakages are quite accurate. The errors quoted are maximum for concentration or current in the system.

Six simple problems are examined. First we consider a single region slab containing two isotopes. The second isotope is stable and has a source term resulting from

TABLE I  
One-Region, Two-Isotope Slab Problem

Isotope <i>ID</i> No.	Diffusion coefficient (cm <sup>2</sup> /sec)	Decay constant (sec <sup>-1</sup> )	Initial concentration (atoms/cm <sup>3</sup> )	Source (atoms/ cm <sup>3</sup> /sec)
1	1.0	4.0	0.0	4.0
2	1.0	0.0	0.0	$L_1 C_1$

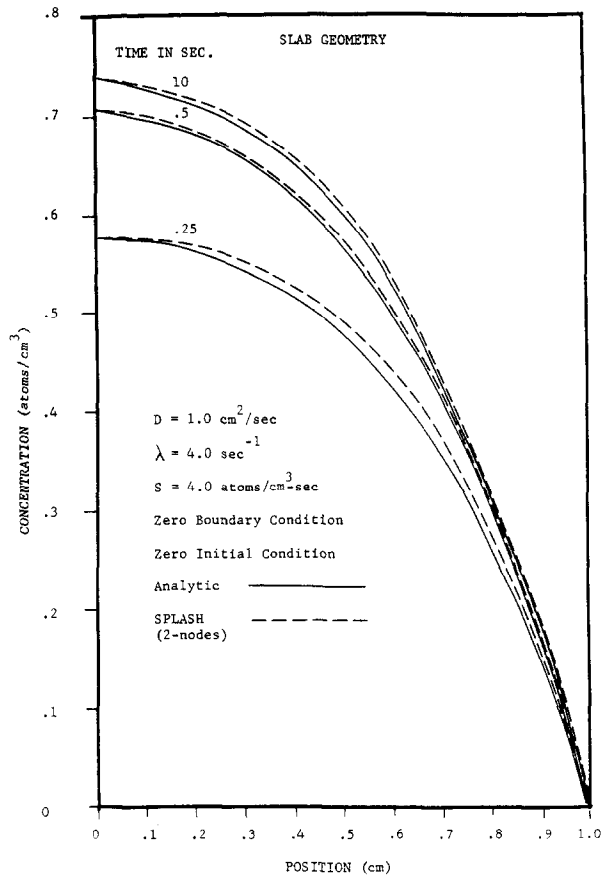


FIG. 1. Concentration in a one-region slab with diffusion and decay.

the decay of the first isotope, as described in Table I. These parameters were chosen for comparison with other investigations [3, 12]. If we examine only the solution for the first isotope, then the analytic solution is readily evaluated for a homogeneous Dirichlet boundary condition [3, 13]. The two-node solutions (a node at the center and the outside) at  $t=0.25, 0.50,$  and  $10.0$  s are compared in Fig. 1. The spatial error relative to the analytic solution at  $t=10$  s, the time of maximum error, is compared in Fig. 2 for 2, 3, and 4 nodes. The approximate maximum errors with 2, 3, and 4 nodes are 2.5, 0.3, and 0.01%, respectively.

The two-isotope two-node solution is illustrated in Fig. 3 at  $t=10$  sec. The percentage errors compared to the analytical solutions are shown in Fig. 4. The maximum error occurs between the nodal values, and, as the number of nodes increases, the error approaches zero, typically as  $O(h^6)$ .

The viability of the method to correctly determine integral quantities was examined. A comparison of the computed and analytic values of the volume

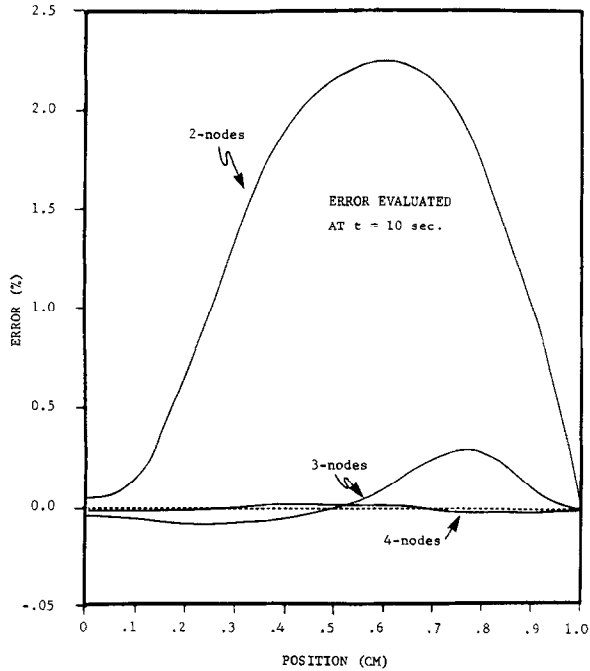


FIG. 2. Error versus position in the one-region slab problem.

integral of the time rate of change of the concentration is given in Table II. The analytic, conservative, and non-conservative formulations are compared in the two-node approximation. Compared to the analytic solution the conservation results are accurate over several orders of magnitude in time, while the non-conservation results are not. For all cells, this integral must vanish identically for steady state solutions.

If the conservation formulation is not utilized, a false prediction of a time rate of change of the volume integral of the concentration is made in the steady state domain. Of course, the errors made by the non-conservative solution diminish as the number of nodes is increased, but then the basic advantage of a variational (Galerkin) method is lost, namely, obtaining an accurate answer rapidly with few nodes. Consequently, the conservation constraint is necessary and preferred.

Next, we consider two simple spherical pure diffusion problems. Figure 5 illustrates a pebble bed reactor spherical fuel ball model, defined in Table III, which is used to compare the SPLASH and DASH computations. First, a one-region sphere is considered with  $a = 3$  cm,  $D = 1.06 \times 10^{-6}$  cm<sup>2</sup>/sec, and  $S = 10^{15}$  atoms/cm<sup>3</sup>-sec. This corresponds to the two-region problem treated below with the first-region properties throughout. Figure 6 illustrates the comparison of the 3-node SPLASH and the ONESPHERE [3] analytic solutions. The 3-node SPLASH solution is within 3% of the analytic solution for all times. Analytic accuracy is

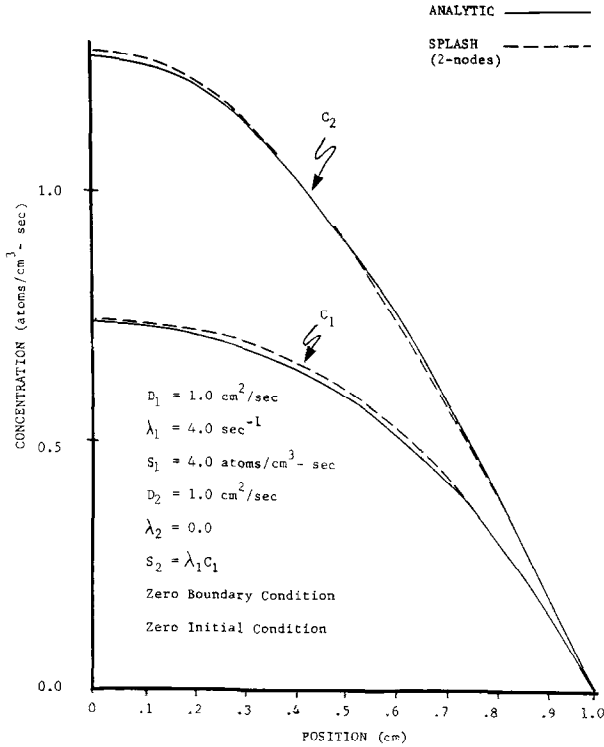


FIG. 3. Two-isotope diffusion with decay in slab geometry.

obtained by 2-node SPLASH solutions at 300 days. For 5 or more nodes, the solutions are graphically indistinguishable. The percentage errors for 3 and 5 nodes are shown in Fig. 7 at  $t = 3$  days, the time of maximum error. The DASH FD solutions, also performed with the exponential matrix method for the time solutions, had a 1% maximum error in concentration at 3 days and a 1.6% error in the current at the outside boundary using 16 carefully positioned mesh cells [3]. SPLASH used 14 equations for 5 nodes and had a maximum error of 0.2%. The SPLASH solution is valid throughout the cell, while the DASH solution is only defined as an averaged value at a finite number of points. Thus, for a similar computing investment, SPLASH will yield a much more accurate solution than the corresponding FD method, all else being equal. SPLASH additionally offers the possibility of analytic accuracy when the analytic solution is spatially cubic or lower order, due to the trial functions employed.

Second, the SPLASH and TWOSPHERE [3] analytic solution of the two-region problem are compared in Fig. 8. For the 3-node numerical solution, one node was placed at the center, one node at the boundary between the two regions, and one node at the outside boundary. Figure 9 illustrates the percentage error compared

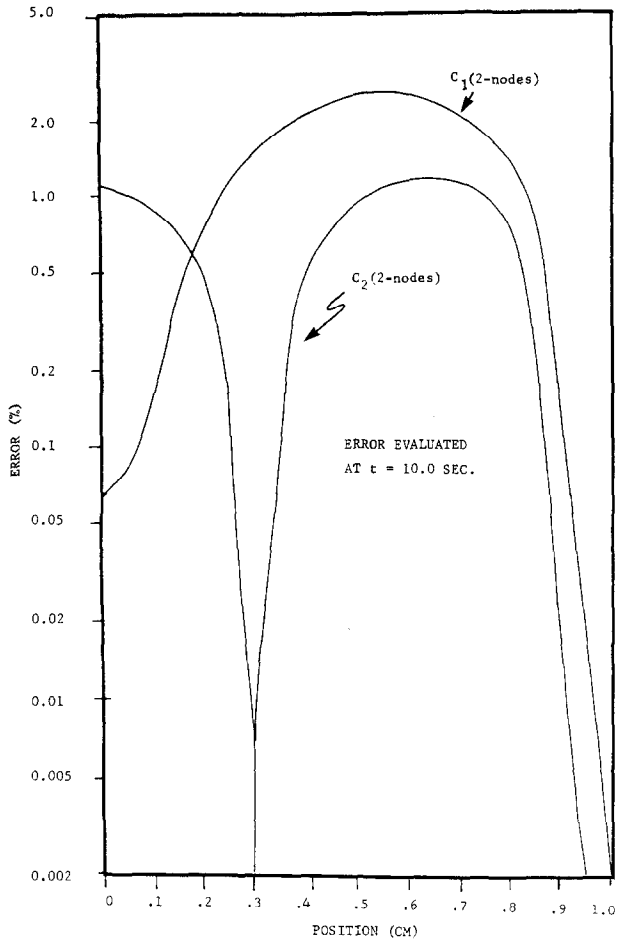


FIG. 4. Error versus position in the two-isotope slab diffusion problem.

TABLE II

Comparison of  $\int dC/dt dV$  with and without Conservation

Time (sec)	Analytic	Conservation (2 nodes)	Non-conservation (2 nodes)
0.25	0.6437	0.6369	0.7367
0.375	0.2868	0.2835	0.3754
0.50	0.1278	0.1263	0.2147
1.00	0.00504	0.00498	0.0907
10.00	0.0	0.0	0.08561
100.0	0.0	0.0	0.08561

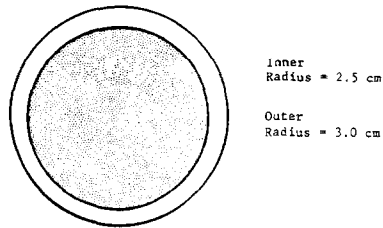


FIG. 5. Pebble bed reactor spherical fuel ball.

with the analytic solution for 3, 5, and 7 nodes at  $t = 3$  days, which was the time of maximum error. The maximum spatial errors for 3, 5, and 7 nodes are 5.0%, 0.25%, and 0.08%, respectively. The 5% error with 3 nodes is reduced significantly by the placement of one additional node in the inside region.

Table IV summarizes the maximum errors compared with the analytical solution in concentration and flux (at the outside surface) with 3 nodes at various times. The 3-nodes SPLASH flux error is comparable to DASH FD results at  $t = 3$  days using 18 carefully adjusted cells, and orders of magnitude better for longer times. This improved accuracy with only one-third the total number of equations is important in numerical estimation of the fission products leaking from such fuel elements [3].

As a more complete test of the SPLASH solution method, the two-region two-group time dependent neutron diffusion problem in slab and spherical geometry was evaluated at late times and the neutron fluxes were compared to critical eigenvalue solutions obtained analytically and from a steady state conservational variational method [7]. For this purpose we supply an initial flux distribution, and evaluate the solution at a late time. These two group problems produce completely coupled multicomponent multiregion equations [14, 15]. The nuclear parameters given in Table V produce thermal flux peaking in the reflector near the core interface.

TABLE III

Two-Region Spherical Diffusion Parameters

Inner radius (region 1)	$a = 2.5$ cm
Outer radius (region 2)	$b = 3.0$ cm
Diffusion coefficients	
region 1	$D_1 = 1.02 \times 10^{-6}$ cm <sup>2</sup> /sec
region 2	$D_2 = 4.34 \times 10^{-7}$ cm <sup>2</sup> /sec
Sources	
region 1	$S_1 = 10^{15}$ atoms/cm <sup>3</sup> -sec
region 2	$S_2 = 10^{15}$ atoms/cm <sup>3</sup> -sec
Zero boundary condition	$C(b, t) = 0.0$
Zero initial condition	$C(r, 0) = 0.0$

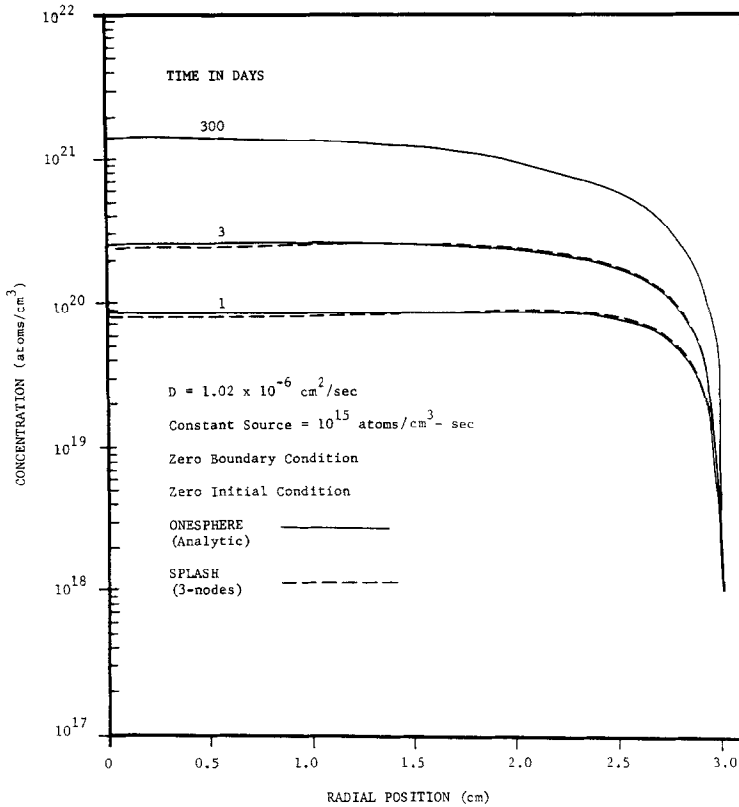


FIG. 6. Concentration in a one-region sphere.

First, for the slab reactor with a 25-cm reflector, the analytical critical half-thickness is 7.987788 cm. The SPLASH 5-node neutron flux steady state solution is compared with the analytic solution determined by the critical determinant method [14] in Fig. 10, where the thermal flux peaking is exhibited with 5 nodes. The maximum fast flux error was 0.25% in the core and 5.2% in the reflector, while the maximum thermal flux error was 1.7% in the core and 5% in the reflector, which is due to the rather large (12.5 cm) spacing in the reflector. Comparison of SPLASH with the steady state conservational variational code, TRIO [7], indicates that both calculations yield comparable fluxes with the same input and node placement. An 11-node steady state variational solution to this problem is an order of magnitude more accurate than DASH with 50-mesh cells. For the critical slab the DASH maximum errors with 50-mesh cells are 0.33 and 0.60% for the fast and thermal fluxes, respectively.

Second, for the spherical reactor with a 25-cm reflector, the analytical critical radius is 21.91046 cm. The SPLASH 5-node neutron flux steady state solution is

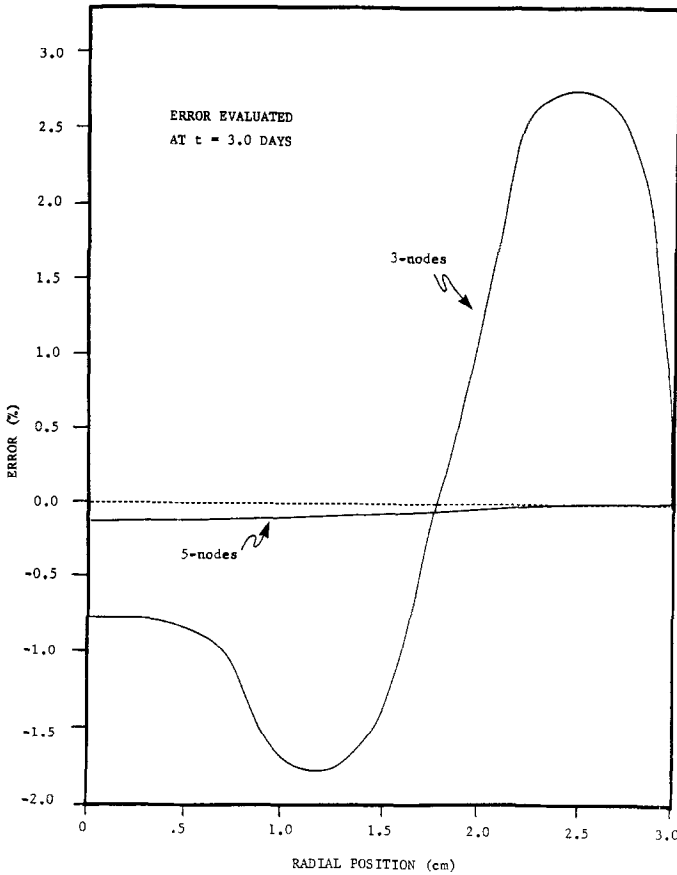


FIG. 7. Error versus position in the one-region sphere.

compared with the analytic solution in Fig. 11. The thermal peaking is weak in a critical sphere and SPLASH could not follow it completely with just 5 nodes when the mesh cells are 12.5 cm. The maximum fast flux error was 1.3% in the core and 3.5% in the reflector, while the maximum thermal flux error was 4.6% in the core and 16.6% in the reflector. The maximum error occurs in the vicinity of the thermal peaking in the reflector where the coarse 12.5-cm spacing precluded fine resolution of the peaking phenomena. An 11-node steady state solution to this problem is an order of magnitude more accurate than DASH with 50-mesh cells. For the critical sphere, the DASH maximum errors with 50-mesh cells are 0.74 and 1.25% for the fast and thermal fluxes, respectively.

These neutronic results indicate that the SPLASH conservation variational method yields accurate results with just a few nodes, that the thermal peaking

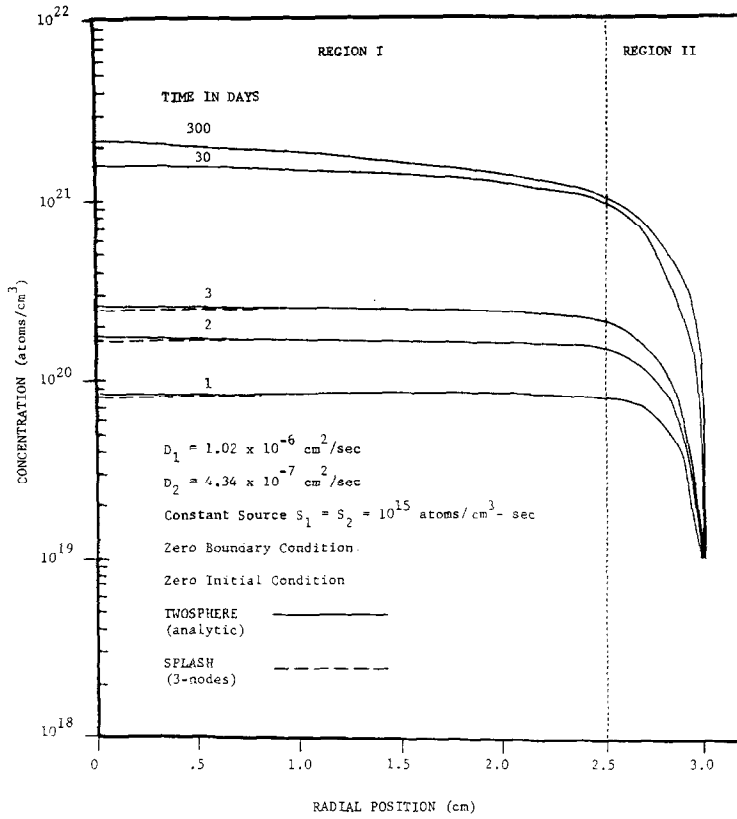


FIG. 8. Concentration in a two-region sphere.

phenomena can be predicted with as few as 5 nodes, and that better accuracy is obtained with approximately half the total number equations used by FD methods. In these comparisons the ASH solution method was used for both the variational and FD time dependent solutions.

When the SPLASH program is run on the CRAY of CDC-205 computers, with only minor subroutine modifications, 98% vectorization is obtained. The optimized running time of the exponential matrix method increases proportional to  $n^{2.5}$ , where  $n$  is the total number of equations. This suggests that a speed improvement factor of 16 over the DASH FD method might be obtained by the conservation variational method in SPLASH. We note that although the SPLASH matrix size for specified accuracy is smaller than the DASH FD matrix, the SPLASH submatrices are completely filled, whereas the DASH submatrices are tridiagonal. The increased SPLASH accuracy for sparse node placement is probably due to the additional coupling in the matrix elements, but this coupling feature *does not affect* the exponential matrix computation time. Additionally, even for a solution with 300

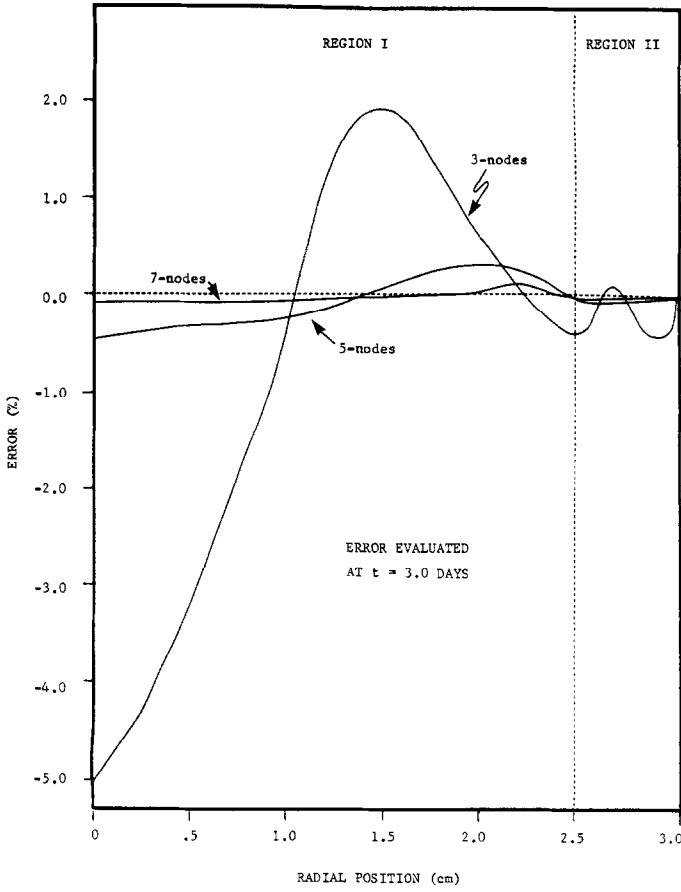


FIG. 9. Error versus position in the two-region sphere.

TABLE IV

Two-Region Sphere Maximum Error Comparisons: 3 Nodes

Time (days)	Concentration (% Error)	Flux( $r = b, t$ ) (% Error)
1.0	2.019	1.072
3.0	5.042 <sup>a</sup>	1.043 <sup>b</sup>
30.0	0.183	0.021
300.0	$4.8 \times 10^{-8}$	$3.0 \times 10^{-7}$

<sup>a</sup> Error with DASH finite difference code using 18 carefully adjusted mesh cells = 3.4% at 3 days[3].

<sup>b</sup> Error with DASH finite difference code using 18 carefully adjusted mesh cells = 2.7% at 3 days[3].

TABLE V  
Nuclear Data for Two-Group Criticality Problem

Parameter	Group 1		Group 2	
	Core	Reflector	Core	Reflector
Diffusion coefficient [cm]	1.13	1.13	0.16	0.16
Removal cross section [cm] <sup>-1</sup>	0.0419	0.0419	0.06	0.0197
Fission cross section [cm] <sup>-1</sup>	0	0	0.03415	0.0
$\nu$	0	0	2.44	0.0
$\Sigma_{1 \rightarrow 2}$	0.0412	0.0412		
$\Sigma_{2 \rightarrow 1}$	$\nu \Sigma_{f2}$	0.0		

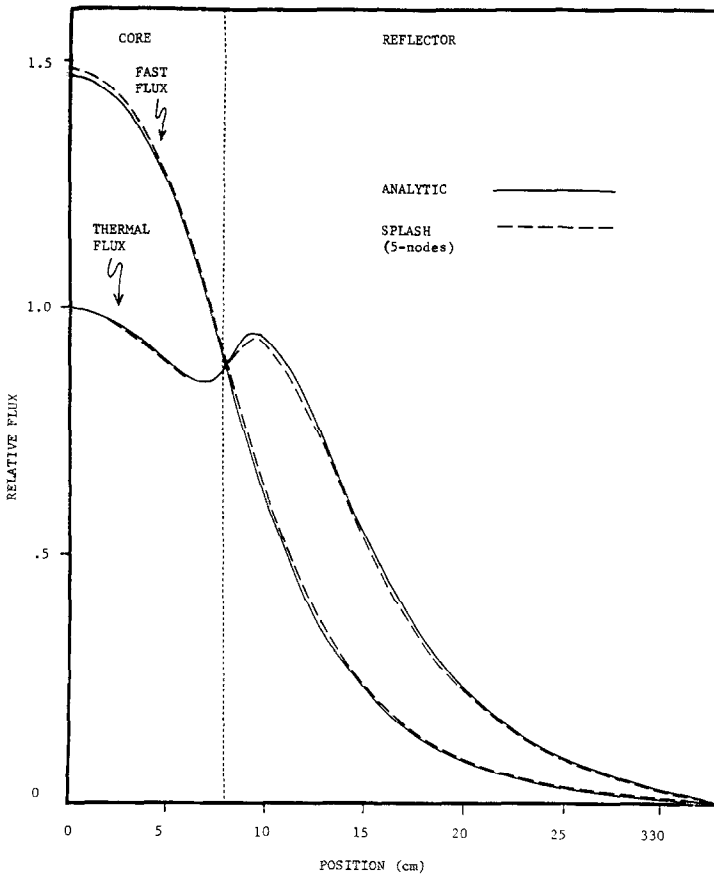


FIG. 11. Two-group flux profile in a critical reflected sphere reactor.

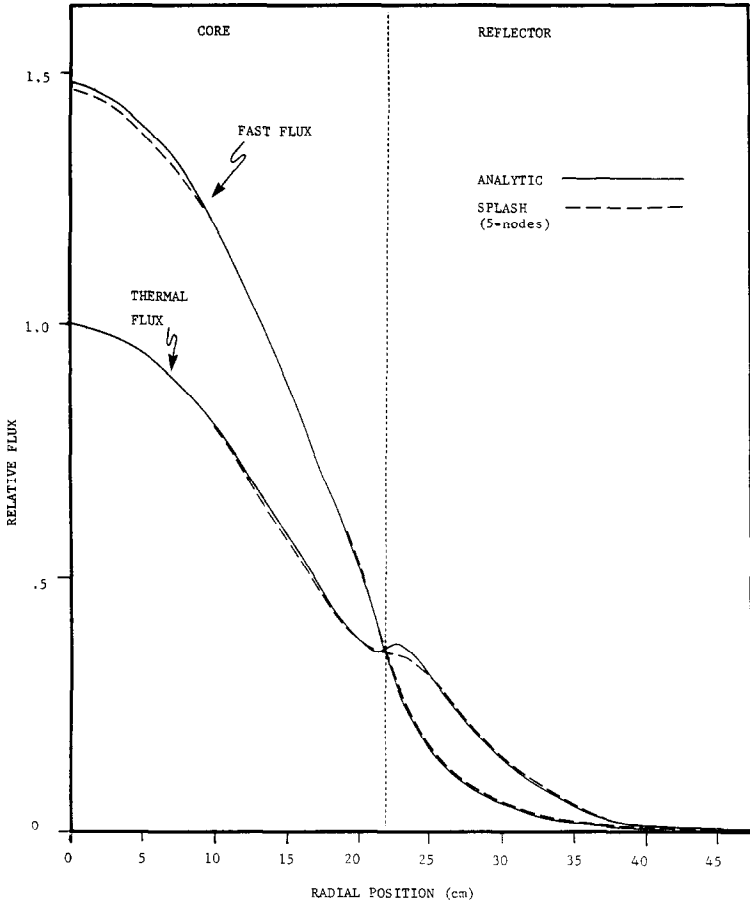


FIG. 10. Two-group flux profile in a critical reflected slab reactor.

nodes at 50 days, extending the solution to  $5 \times 10^{10}$  days (a large, but valid steady state estimate) resulted in less than a factor 2 increases CPU time, which illustrates the economic advantages of scaling and recursion by powers of 2.

### CONCLUSIONS

For the same accuracy level, the SPLASH conservation variational method achieves an accurate solution with significantly less computing effort than finite difference methods.

One- and two-region, one- and two-isotope solutions with decay and pure diffusion were compared with analytical solutions in slab and spherical geometries. As

the number of nodes is increased, the maximum error (which occurs between nodal points) apparently decreases as  $O(h^6)$  for the problems addressed. This improved convergence rate occurs possibly because of the integral conservation constraints imposed on the solution. Late time SPLASH solutions approach cubic order steady state solutions exactly.

Additionally, SPLASH and DASH were applied to the solution of the time dependent two group neutron diffusion equations for a critical system. Excellent agreement with the steady state critical eigenvalue results were obtained for the neutron flux and current.

Comparison with DASH FD diffusion solutions, using the exponential matrix method, indicates that SPLASH can evaluate the solution to time dependent multicomponent diffusion decay problems more accurately with less than one-half as many coupled equations. This implies roughly an order of magnitude computational speed improvement is possible with SPLASH for the same accuracy. Vectorization is implemented readily.

If the conservation Lagrange multiplier constraints are *not* used (as is typical in some codes), the non-conserving aspects of the solution are apparent. The volume integral,  $\int dC/dt dV$ , when calculated by substituting the solution into the diffusion equation, may be predicted quite erroneously. As the non-conservation solution approaches steady state (when  $\int dC/dt dV$  should approach zero), the predicted  $\int dC/dt dV$  remains large. Computation at later times yields the same steady state concentration solution, but, again, an erroneous predicted  $\int dC/dt dV$  value. Although the non-conservation solution method yields more accurate conservation predictions with a considerably increased number of nodes per region, this practice is uneconomical.

The conservation solution, on the other hand, correctly and accurately approaches the steady state with a minimal number of nodes. Additionally,  $dC/dt$  approaches zero and is in good agreement with the analytic solution at all times. It seems physically and computationally important that the numerical solutions to a problem satisfy the prescribed differential equations, the boundary conditions, and particle conservation!

#### APPENDIX: MATRIX ELEMENTS FOR THE VARIATIONAL METHOD

We define the integral

$$\langle a(p) \rangle_i = k(c) \int_0^1 dp (K_i p + r_i)^c a(p),$$

where  $k(c) = 1, 2\pi,$  and  $4\pi$  for  $c = 0, 1,$  and  $2$  in slab, cylindrical, and spherical geometry, respectively.

The matrix elements for the variational diffusion problem, Eq. 13 in the text, are

$$[T] = \begin{bmatrix} e_1 & f_1 & 0 & \cdot & \cdot & \cdot \\ f_1^T & e_2 & f_2 & 0 & \cdot & \cdot \\ 0 & f_2^T & e_3 & f_3 & 0 & \cdot \\ \cdot & \cdot & \cdot & \cdot & \cdot & \cdot \\ \cdot & \cdot & \cdot & \cdot & \cdot & \cdot \\ \cdot & \cdot & 0 & f_{n-1}^T & e_n & f_n \\ \cdot & \cdot & 0 & 0 & f_n^T & e_{n+1} \end{bmatrix},$$

$$-[A] = \begin{bmatrix} b_1 & c_1 & 0 & \cdot & \cdot & \cdot \\ a_1 & b_2 & c_2 & 0 & \cdot & \cdot \\ 0 & a_2 & b_3 & c_3 & 0 & \cdot \\ \cdot & \cdot & \cdot & \cdot & \cdot & \cdot \\ \cdot & \cdot & \cdot & \cdot & \cdot & \cdot \\ \cdot & \cdot & 0 & a_{n-1} & b_n & c_n \\ \cdot & \cdot & 0 & 0 & a_n & b_{n+1} \end{bmatrix},$$

and the elements  $a_k$ ,  $b_k$ ,  $c_k$ ,  $e_k$ , and  $f_k$  are  $3M \times 3M$  matrices.

The individual matrix elements and their forms are summarized below for  $M = 1$ , where we have assumed  $[D] = D_{n,m}d_{n,m}$ :

$$e_{i,11} = K_{i-1} \langle s_0^2(p) \rangle_{i-1} + K_i \langle s_0^2(1-p) \rangle_i,$$

$$e_{i,12} = e_{1,21} = (K_{i-1}^2 [D(r_{i-})]^{-1}) \langle s_0(p) s_1(p) \rangle_{i-1} \\ - (K_i^2 [D(r_{i+})]^{-1}) \langle s_0(1-p) s_1(1-p) \rangle_i,$$

$$e_{i,22} = (K_{i-1}^3 [D(r_{i-})]^{-2}) \langle s_1^2(p) \rangle_{i-1} + (K_i^3 [D(r_{i+})]^{-2}) \langle s_1^2(1-p) \rangle_i,$$

$$e_{i,31} = e_{i,13} = K_i \langle s_0(1-p) \rangle_i,$$

$$e_{i,32} = e_{i,23} = -(K_i^2 [D(r_{i+})]^{-1}) \langle s_1(1-p) \rangle_i,$$

$$e_{i,33} = 0,$$

$$f_{i,11} = K_i \langle s_0(1-p) s_0(p) \rangle_i,$$

$$f_{i,12} = (K_i^2 [D(r_{i+1-})]^{-1}) \langle s_0(1-p) s_1(p) \rangle_i,$$

$$f_{i,13} = 0,$$

$$f_{i,21} = -(K_i^2 [D(r_{i+})]^{-1}) \langle s_1(1-p) s_0(p) \rangle_i,$$

$$f_{i,22} = -(K_i^3 [D(r_{i+}) D(r_{i+1-})]^{-1}) \langle s_1(1-p) s_1(p) \rangle_i,$$

$$f_{i,23} = 0,$$

$$f_{i,31} = K_i \langle s_0(p) \rangle_i,$$

$$f_{i,32} = (K_i^2 [D(r_{i+1-})]^{-1}) \langle s_1(p) \rangle_i,$$

$$f_{i,33} = 0,$$

$$b_{i,11} = \langle ([D_{i-1}(p)]/K_{i-1}) s_0'^2(p) + K_{i-1} [L_{i-1}(p)] s_0^2(p) \rangle_{i-1} \\ + \langle ([D_i(p)]/K_i) s_0'^2(1-p) + K_i [L_i(p)] s_0^2(1-p) \rangle_i,$$

$$b_{i,12} = b_{1,21} = \langle [D(r_{i-})]^{-1} ([D_{i-1}(p)] s_0'(p) s_1'(p) \\ + K_{i-1}^2 [L_{i-1}(p)] s_0(p) s_1(p)) \rangle_{i-1} \\ - \langle [D(r_{i+})]^{-1} ([D_i(p)] s_0'(1-p) s_1'(1-p) \\ + K_i^2 [L_i(p)] s_0(1-p) s_1(1-p)) \rangle_i$$

$$b_{i,13} = b_{i,31},$$

$$b_{i,22} = [D(r_{i-})]^{-2} K_{i-1} \langle [D_{i-1}(p)] s_1'^2(p) + K_{i-1}^3 [L_{i-1}(p)] s_1^2(p) \rangle_{i-1} \\ + [D(r_{i+})]^{-2} K_i \langle [D_i(p)] s_1'^2(1-p) + K_i^3 [L_i(p)] s_1^2(1-p) \rangle_i,$$

$$b_{i,23} = b_{i,32},$$

$$b_{i,31} = K_i \langle [L_i(p)] s_0(1-p) \rangle_i,$$

$$b_{i,32} = -A_i^* - K_i^2 [D(r_{i+})]^{-1} \langle [L_i(p)] s_1(1-p) \rangle_i,$$

$$b_{i,33} = 0,$$

$$c_{i,11} = -\langle ([D_i(p)]/K_i) s_0'(1-p) s_0'(p) - K_i [L_i(p)] s_0(1-p) s_0(p) \rangle_i,$$

$$c_{i,12} = -[D(r_{i+1-})]^{-1} \langle [D_i(p)] s_0'(1-p) s_1'(p) - K_i^2 [L_i(p)] s_0(1-p) s_1(p) \rangle_i,$$

$$c_{i,13} = 0,$$

$$c_{i,21} = [D(r_{i+})]^{-1} \langle [D_i(p)] s_1'(1-p) s_0'(p) - K_i^2 [L_i(p)] s_1(1-p) s_0(p) \rangle_i,$$

$$c_{i,22} = [D(r_{i+}) D(r_{i+1-})]^{-1} \langle K_i [D_i(p)] s_1'(1-p) s_1'(p) \\ - K_i^3 [L_i(p)] s_1(1-p) s_1(p) \rangle_i,$$

$$c_{i,23} = 0,$$

$$c_{i,1} = K_i \langle [L_i(p)] s_0(p) \rangle_i,$$

$$c_{i,32} = A_{i+1}^* + K_i^2 [D(r_{i+1-})]^{-1} \langle [L_i(p)] s_1(p) \rangle_i,$$

$$c_{i,33} = 0,$$

and

$$a_{i,jk} = c_{i-1,kj}, \quad 1 \leq j, k \leq 3,$$

where  $A_i^* = A_i/k(c)$  and  $F'(p) = \partial f(p)/\partial p$ . The corresponding expressions for  $M > 1$  are straightforward.

## REFERENCES

1. S. NAKAMURA, "Computational Methods in Engineering and Science with Applications to Fluid Dynamics and Nuclear Systems," Wiley, New York, 1977.
3. C. E. APPERSON, JR., C. E. LEE, AND L. M. CARRUTHERS, "DASH: A Multicomponent Time-Dependent Concentration Diffusion with Radioactive Decay Program," Los Alamos National Laboratory Report NUREG/CR-0776, LA-7793-MS, 1979.
3. C. E. HORTON, "A Model of the Fission Product Release from a Typical Operating Pebble Bed Reactor," Master of Engineering Report, Department of Nuclear Engineering, Texas A & M University, College Station, Tex. 1980.
4. C. E. LEE AND C. E. APPERSON, JR., *Trans. Amer. Nucl. Soc.* **30** (1978), 253.
5. P. M. MORSE AND H. FESHBACH, "Methods for Theoretical Physics," Vol. I, McGraw-Hill, New York, 1953.
6. J. P. HENNART, *Nucl. Sci. Eng.* **50** (1973), 185-199.
7. C. E. LEE, W. C. P. FAN, AND R. L. BRATTON, *Ann. Nucl. Energy*, **11** (1984), 493-515.
8. C. E. LEE, "Proceedings of the International Conference on Nuclear Waste Transmutation, Austin, Texas," pp. 651-670 (July 1980).
9. F. R. GANTMACHER, "The Theory of Matrices," Chelsea, New York, 1960.
10. C. E. LEE AND B. C. WILSON, *Trans. Amer. Nucl. Soc.* **39** (1981), 961.
11. B. C. WILSON, "Solution of the Time-Dependent Diffusion Equation Using a Conservation Variational Method," M. S. thesis, Texas A & M University, 1981.
12. C. E. LEE AND J. W. DURKEE, "Multiregion Concentration Diffusion Coefficient Determination Using Davidson's Variable Metric Method," *Nucl. Technol.* **69** (1985), 218-235.
13. H. S. CARSLAW AND J. C. JAEGER, "Conduction of Heat in Solids," 2nd ed., Oxford Univ. Press, Oxford, 1979.
14. J. R. LAMARSH, "Nuclear Reactor Theory," Addison-Wesley, Reading, Mass. 1972.
15. J. J. DUDERSTADT AND L. J. HAMILTON, "Nuclear Reactor Analysis," Wiley, New York, 1976.